

# Geostationary Earth Radiation Budget (GERB) Data

J E Russell<sup>(1)</sup>, J E Harries<sup>(1)</sup>, N Clerbaux<sup>(2)</sup>

<sup>(1)</sup>*Space and Atmospheric Physics, Imperial College, London SW7 2BZ, UK*

<sup>(2)</sup>*Royal Meteorological Institute Belgium, Brussels, Belgium.*

## Abstract

The Geostationary Earth Radiation Budget (GERB) instrument on METEOSAT-8 is making the first measurements of the Earth's radiation budget from geostationary orbit. The first validated GERB Edition 1 products were released to the scientific community via the ggsps archive (<http://ggsps.rl.ac.uk>) earlier this year. This paper summaries the calibration accuracy and validation results for these Edition 1 products. Absolute accuracy for reflected solar and emitted thermal unfiltered radiances are determined as 2.25% and 0.96% respectively. Angularly matched radiance comparison with CERES (FM2) measurements show GERB reflected shortwave radiances to be on average 5% higher and emitted thermal radiances to be 1% lower than the corresponding CERES quantities. A comparison between the GERB and CERES fluxes shows that the GERB reflected solar fluxes are on average 7% higher than CERES and the emitted thermal fluxes are 1% lower than CERES.

## INTRODUCTION

The first Geostationary Earth Radiation Budget (GERB) [1] was launched as an instrument of opportunity onboard Meteosat-8 in August 2002 and made the first ever observations of the broadband reflected solar and emitted thermal energy from geostationary orbit in December 2002. Since this time it has been operating almost continuously, providing near-real time (NRT) shortwave and longwave top of the atmosphere radiances and fluxes every 15 minutes for the region 60W to 60E, 60N to 60S, with a spatial resolution at the sub-satellite point of 44.6 km (N-S) by 39.3 km (E-W).

The unique measurements that GERB makes allow the study of forcing and feedback mechanisms on the short time scales that are important in many cases, and in turn to provide improved understanding of these mechanisms to determine inter-annual and longer term climate variability.

A series of 4 GERB instruments will be flown sequentially on each of the Meteosat Second Generation (MSG) satellites along with the prime meteorological instrument the Scanning Enhanced Visible and Infrared (SEVIRI) ([2] and [3]). These should provide a continuous GERB data record spanning at least a decade.

A thorough understanding of the accuracy of the measurements, supported by extensive validation is necessary to allow the data to be appropriately used. The first validated Edition 1 GERB data products were released to the scientific community earlier this year. In this paper we summaries the calibration accuracy for this first edition and report the validation results.

## PROCESSING AND CALIBRATION ACCURACY

The absolute accuracy aims for the GERB products are 1% (of the typical full scale radiance) for the emitted thermal (hereafter referred to as LW) and the reflected solar (hereafter referred to as SW) radiances, and 0.1 GERB pixel for the geolocation. The theoretical accuracy of the edition 1 GERB products does not meet all of these targets due to known issues which we plan to resolve in future releases. Below is a summary of our current understanding of the theoretical accuracy of the GERB radiances and geolocation.

### Unfiltered radiances

Table 1 summarises the approximate magnitudes of each of the error contributions affecting the absolute accuracy of the GERB unfiltered radiances, and determines an RMS combination of the contributions to derive an overall accuracy assessment for the unfiltered radiances. Errors are quoted as a percentage where a fixed error in the quantities corresponds to a fixed fractional error in the unfiltered radiances, independent of the magnitude of the unfiltered radiances. Where a fixed error causes a fixed radiance error on the unfiltered radiances, this is quoted as a percentage of the typical full scale radiances which are taken

to be  $240 \text{ Wm}^{-2}\text{sr}^{-1}$  for the SW and  $77 \text{ Wm}^{-2}\text{sr}^{-1}$  for consistency with the accuracy requirements. No random errors, including those that may be systematic for a particular scene type, are considered in table 1.

Errors due to the accuracy of the calibration sources and spectral response are determined as the combined effect of 1SD level spectrally random and spectrally systematic uncertainties on the sources and response measurements. For the spectral response the errors quoted are the worst case effect in  $\text{Wm}^{-2}\text{sr}^{-1}$  expressed as a percentage of the full scale, that the uncertainty causes over a wide variety of simulated Earth scenes,. As SEVIRI is used to unfilter the GERB radiances, the effect of the quoted SEVIRI calibration uncertainty is also determined and the simulated worst case effect of a SEVIRI inter-channel calibration error at a  $\pm 5\%$  level is quoted for the LW and SW radiances. For the SW a worst case effect is an overestimation of the unfiltering factor by 0.8% if the errors on SEVIRI  $0.6\mu\text{m}$  is  $+5\%$  and on  $0.8\mu\text{m}$  and  $1.6\mu\text{m}$  is  $-5\%$ . For the longwave the worst case is found to be an overestimation of the unfiltering factor by 0.09% for  $-5\%$  on  $6.2\mu\text{m}$ ,  $7.3\mu\text{m}$ ,  $12\mu\text{m}$  and  $13.4\mu\text{m}$  SEVIRI channels and  $+5\%$  on  $8.7\mu\text{m}$  and  $10.8\mu\text{m}$ .

Random errors are considered in table 2. This table includes contributions from detector noise, interpolation and unfiltering. Uncertainties due to these sources are stated as percentages of the typical full scale radiances are before. The estimated 1 standard deviation (1 SD) random error in geolocation accuracy is stated in terms of GERB pixels. It should be noted that geolocation errors will lead to errors in the assigned filtered radiances for a given location, and additional errors due to a mismatch with SEVIRI in the unfiltering factor and the radiance to flux conversion factors. Whilst random in origin, unfiltering and geolocation errors can lead to systematic errors in radiances and fluxes ascribed to a particular scene type.

| Error source  | Reflected solar                      | Emitted thermal (night)     | Emitted thermal (day)       |
|---|--------------------------------------|-----------------------------|-----------------------------|
| Calibration sources absolute accuracy (1 SD uncertainty values)             | ~0.22%                               | <0.05%                      |                             |
| Calibration sources uniformity (full range over region used)                | < 0.5%                               | Small                       |                             |
| Spectral response   | 1.9% of typical full scale           | <0.9% of typical full scale | <0.9% of typical full scale |
| Stray light (maximum effect in un-flagged data)                             | <0.25 $\text{Wm}^{-2}\text{sr}^{-1}$ |                             |                             |
|   | <0.1% of typical full scale          | <0.3% of typical full scale |                             |
| Polarisation (Worst case error for a completely linearly polarised source.) | <0.4%                                | Small                       |                             |
| SEVIRI inter-channel calibration  | <1%                                  | <0.1%                       | <0.1%                       |
| RMS combination of above errors   | 2.25%                                | 0.96%                       | 0.96%                       |

**Table 1. Estimates of the ground determined unfiltered radiance bias error sources and magnitudes.**

| Error source                | Reflected solar             | Emitted thermal (night)     | Emitted thermal (day)       |
|-----------------------------|-----------------------------|-----------------------------|-----------------------------|
| Instrument noise            | 0.13% of typical full scale | 0.4% of typical full scale  | 0.6% of typical full scale  |
| Geolocation                 | 0.25 pixel                  |                             |                             |
| Interpolation               | 0.63% of typical full scale | 1% of typical full scale    | 1% of typical full scale    |
| Spectral overlap correction | 0.02% of typical full scale | None                        | 0.08%                       |
| Unfiltering                 | 0.3% of typical full scale  | 0.05% of typical full scale | 0.05% of typical full scale |

**Table 2. Estimates of the random errors on the unfiltered radiance.**

GERB SW fluxes are derived from the GERB SW radiances using the CERES TRMM ADMs as the basis of the radiance to flux conversion [4]. The ADMs which are the basis of the radiance to flux conversions are

statistical in nature and thus a random error will be associated with the instantaneous flux estimates, the 1SD values of these errors are shown in table 3. In addition SEVIRI measurements are employed both for the scene identification required to choose the appropriate SW radiance to flux conversion factor, and in determining the longwave radiance to flux conversion. Thus, the effect of 5% calibration errors on the SEVIRI radiances and inter-channel calibration is also considered. In the SW such an error, if present in the 0.6 $\mu$ m radiances affects the cloudy scene identification used to choose the appropriate CERES ADM. In the LW radiance to flux conversion factors are chosen based on SEVIRI channel radiances and the error shown is the worst case effect of 5% inter-channel calibration errors in the LW on the determination of LW anisotropy factor. All flux errors are additional to the radiance errors already discussed.

| Error source   | Reflected solar  | Emitted thermal                         |
|--|--|---|
| SW ADM   | $\sim 10 \text{ Wm}^{-2}$ random error                               |   |
| LW anisotropy  |  | $\sim 5.5 \text{ Wm}^{-2}$ random error |
| SEVIRI channel calibration and inter-channel calibration | $< 1.2 \text{ Wm}^{-2}$ bias<br>$< 5.6 \text{ Wm}^{-2}$ random error | $< 1 \text{ Wm}^{-2}$ bias              |

**Table 3. Addition error sources and approximate magnitudes to which the SW and LW fluxes are subject (see [4] for validation results on the CERES TRMM ADMs).**

### VALIDATION RESULT SUMMARY:

The CERES instruments [5] flying on the low Earth orbit AQUA and TERRA satellites measure the outgoing longwave and reflected shortwave broad band radiances and fluxes in a similar manner to GERB. Their products have been extensively validated and have stated absolute accuracy of 1.0% for the shortwave 0.5% for the longwave radiances. The GERB ARG unfiltered radiances and fluxes have been compared to the CERES FM2 SSF rev 1 unfiltered radiances and fluxes. Results shown here are for the GERB V998 validation reprocessing data set, consisting of 21-27<sup>th</sup> June and 11<sup>th</sup>-17<sup>th</sup> December 2004. This processing version has the same science processing as the Edition 1 release GERB data.

### Radiances

GERB and CERES FM2 SSF rev 1 radiances are matched for time, location and viewing angle. Matched data have viewing angles within 5° of each other and the CERES acquisition time must be no more 170 seconds from the acquisition time for the relevant GERB ARG column. Only data with GERB viewing zenith angles  $< 65^\circ$  for the SW and  $< 80^\circ$  for the longwave are retained and solar zenith angles are also required to be  $< 80^\circ$  for the SW comparison.

Comparison of the two datasets indicates that GERB and CERES LW radiances are in good agreement but the CERES FM2 SW radiances are generally lower than GERB's. A linear fit between the two sets of matched measurements yields a gradient of 1.002 and intercept of  $+ 3.5 \text{ Wm}^{-2}\text{sr}^{-1}$  for the SW and a gradient of 1.0005 and intercept of  $-1.8 \text{ Wm}^{-2}\text{sr}^{-1}$  for the LW. To derive a mean ratio and associated uncertainty, the mean radiance for each day of GERB and CERES points is calculated and the ratio of these two mean values determined. The mean and standard deviation of the ratio is then calculated from all the daily ratios. Table 4 shows the mean ratio and an associated 99% confidence uncertainty determined as 3 times the standard deviation divided by the square root of the number of days.

Figure 1 shows the ratio of the average GERB and CERES radiances for matched data binned according to observed GERB radiance. Results are shown for matches obtained with each of the four CERES instruments. As can be seen from this figure and from some scene dependence is seen in the radiance comparisons. For the SW agreement between GERB and CERES (in percentage terms) is better for bright scenes than for dark scenes. As well as being evident from figure 1 this is also seen in the FM2 comparison results shown in table 4 where it is exhibited as a higher SW ratio for the darker ocean than for cloud or bright desert. For the LW whilst comparisons between GERB and CERES FM2 and FM3 data show no apparent scene dependent effects, comparison between the GERB LW and matched data from FM1 and FM4 show increasing GERB/CERES ratio for the colder GERB scenes.

It should be noted that the scene dependent differences may be affected by the comparison methodology and geolocation errors. For the extreme scenes geolocation errors can lead to systematic effects on the

inferred average radiance. For example geolocation errors can lead GERB scenes identified as ocean to occasionally contain some cloud; in the SW these cloud points will always be brighter than the dark ocean and therefore act to elevate the average SW radiance inferred. The observed scene dependent differences can also be due to systematic uncertainties in the spectral response of the instrument, as in the SW bluer scenes tend to darker scenes and in the LW colder scenes contain a higher proportion of their energy at longer wavelengths than do warmer scenes.

| FM2 (Edition 2) GERB/CERES | SW radiance data                                    | LW radiance data                             |
|----------------------------|---|--|
| June                       | 1.058 ± 0.005 (all sky)<br>1.041 ± 0.013 (overcast) | 0.993 ± 0.001 (day)<br>0.990 ± 0.003 (night) |
| Dec                        | 1.048 ± 0.005 (all sky)<br>1.032 ± 0.005 (overcast) | 0.993 ± 0.001 (day)<br>0.988 ± 0.005 (night) |

| SW GERB/CERES (FM2) radiance ratios for Clear GERB pixels (GERB cloud cover 0%) |               |
|---|---------------|
| Ocean   | 1.144 ± 0.043 |
| Dark Vegetation   | 1.070 ± 0.017 |
| Bright Vegetation   | 1.062 ± 0.010 |
| Dark Desert   | 1.073 ± 0.019 |
| Bright Desert   | 1.059 ± 0.006 |

**Table 4.** Results of radiance comparison for angularly matched and co-located GERB CERES radiances. SSF rev1 radiance data from FM2 (Edition 2) and GERB V998 data are compared. Rev1 all sky correction factor is applied to the CERES SW data. Overcast conditions for the SW are defined as a GERB cloud cover of 100% and optical depth of 7.4 or more.

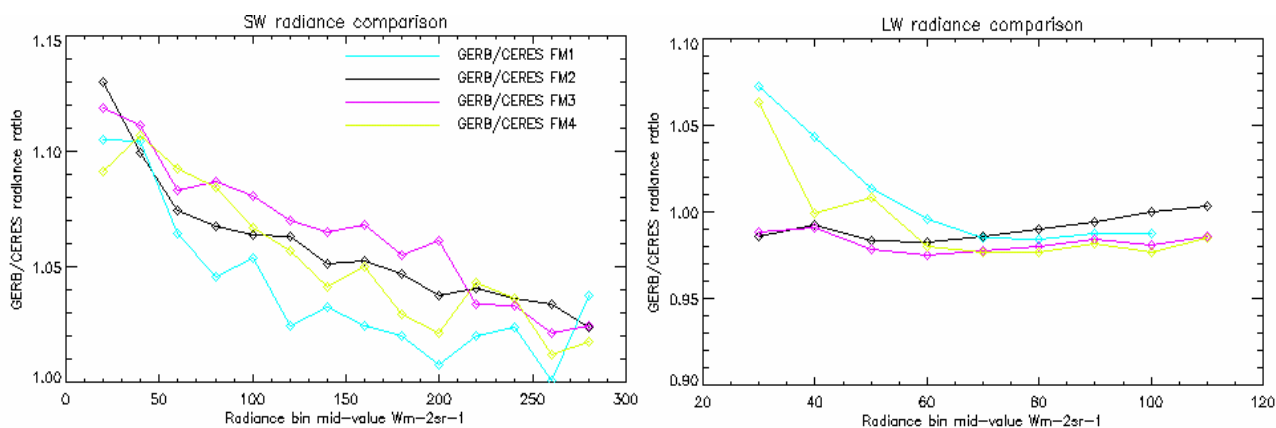


**Figure 1.** GERB/CERES radiance ratios for each of the four CERES instruments as a function of GERB radiance. Ratios determined from average GERB and averages CERES observations in each radiance bin. SW radiance comparison results are shown in the left hand panel and LW radiance comparison results in the right hand panel.

## Fluxes

The GERB V998 level 2 ARG fluxes have also been compared to the CERES FM2 SSF rev 1 fluxes for the periods 21-27<sup>th</sup> June and 11<sup>th</sup>-17<sup>th</sup> December 2004. All CERES flux measurements, within 170 seconds of acquisition time of the relevant ARG column, falling within the GERB footprint are used (note: as fluxes are

now compared there is no need to match viewing geometry). Prior to comparison the CERES SSF fluxes are adjusted from a 20km reference level to a surface reference level.

Each day the mean of GERB and CERES fluxes are determined and the ratio of these means derived. The mean and standard deviation of the ratio is then calculated from the daily ratios. The mean ratio and an associated 99% confidence uncertainty determined as 3 times the standard deviation divided by the square root of the number of days is displayed in table 5.

| GERB/CERES FM2 (Edition 2) flux ratios | SW flux data  | LW flux data   |
|--|---|--|
| June                                   | 1.073 ± 0.004 (all sky)<br>1.054 ± 0.007 (overcast) | 0.991 ± 0.001 (day time)<br>0.987 ± 0.001 (night time) |
| Dec                                    | 1.059 ± 0.004 (all sky)<br>1.044 ± 0.004 (overcast) | 0.992 ± 0.001 (day time)<br>0.987 ± 0.001 (night time) |

| SW GERB/CERES (FM2) flux ratios for Clear GERB pixels (GERB cloud cover 0%) |               |
|---|---------------|
| Ocean   | 1.085 ± 0.018 |
| Dark Vegetation   | 1.072 ± 0.007 |
| Bright Vegetation   | 1.082 ± 0.005 |
| Dark Desert   | 1.081 ± 0.009 |
| Bright Desert   | 1.068 ± 0.007 |

**Table 5. Results of SW and LW flux comparison for co-located GERB CERES fluxes. SSF rev1 flux data from FM2 3 are used. Rev1 all sky correction factor is employed except for clear ocean where rev1 clear ocean factor is employed. Overcast conditions are defined from the GERB scene identification as 100% cloud cover with an optical depth above 7.4.**

In addition, in order to analyse viewing angle dependent and scene dependent differences, an average of the matched points is constructed for each location and smoothed using a 5x5 ARG pixel moving average before being compared to construct a map of the GERB/CERES ratio over the GERB viewing region. The results of these comparisons are shown in figure 2 for the SW all sky and clear sky fluxes and figures 3 for the LW day-time and night-time fluxes.

Over the several days used to accumulate the averages, the CERES data contributing to the average at a given location will have been acquired from a range of viewing angles, whereas due to its geostationary orbit, the GERB viewing geometry remains relatively invariant for each point on the Earth. Thus, whilst view angle dependent errors in the radiance to flux conversion will be much reduced in the CERES average, they are expected to remain in the GERB data at a level comparable to that present in the instantaneous measurements. Therefore the results can highlight the view angle dependent errors in the radiance to flux conversion.

Overall the SW flux comparison show a 1-2% increase in the GERB/CERES ratio compared to the radiance results, although the variation in the ratio with scene is reduced. The discrepancy between the SW radiance comparison and SW flux comparison results can be attributed to a combination of differences in the ADMs (GERB uses the TRMM ADMs and the CERES fluxes used here are derived using the TERRA ADMs) and possible discrepancies in the scene identification. This is evidenced by the fact that comparison of the co-angular GERB CERES flux measurements results in, on average, a 1% difference between the two instruments in the SW anisotropy factors assigned to the SW radiances, which alone would result in an elevation of the GERB/CERES flux ratio by 1% compared to the radiances.

The geographical distribution of the GERB/CERES average flux ratio is shown in figure 2 for the SW. For the all-sky plots, the GERB/CERES SW flux ratio over much of the disk is relatively uniform. Exceptions are seen towards the edge of the disk, particularly for fluxes derived from observations with viewing zenith

angles greater than  $70^\circ$  (indicated by the red ring in the plots). Enhanced SW ratios are seen at the edges of the sunglint region (indicated by a roughly circular black region of missing data) and depressed ratios are observed off the West coast of Africa. As no specific aerosol treatment or radiance to flux conversion is employed, fluxes in the presence of aerosol are expected to be of reduced accuracy, thus the latter effect is likely due to the presence of aerosol as the region of depressed flux is an area where significant aerosol effects are likely. In the clear sky the region of depressed ratios is also clearly visible and arguable a stronger signature, this would be consistent with the aerosol argument as the effect of aerosol would be most significant on the TOA fluxes when no cloud were present. In addition, some enhanced ratios are seen for ocean points close to coastlines and depressed ratio for coastland. These are likely the result of geolocation errors causing land observations to be occasionally included in the average determined for the GERB ocean locations and visa versa.

The average GERB/CERES longwave flux ratios, shown in table 5, are similar to the radiance ratios. The geographical distribution of the GERB/CERES average LW flux ratio is shown in figure 3. A limb darkening effect is apparent in the LW flux comparisons, with GERB fluxes derived from observations at higher viewing angles producing lower ratios than those derived from low view angles. Enhanced ratios are also seen in regions associated with cloud such as the ITCZ; this is believed to be related to a known inability of the GERB LW radiance to flux conversion to account for the anisotropy of high semi-transparent cloud.

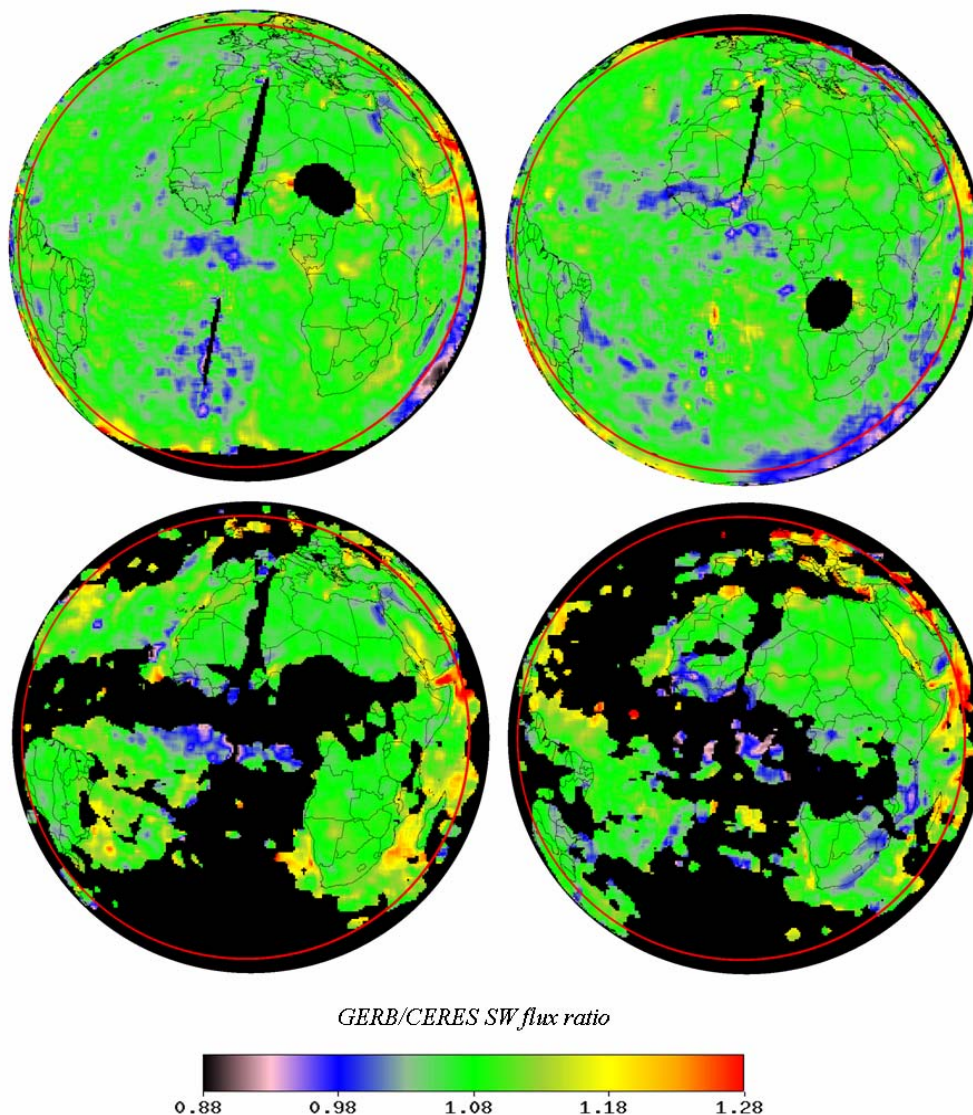


**Figure 2** SW flux comparison for June (left) and December (right). GERB/FM2 ratio shown for all-sky conditions in upper panels and clear sky (identified by GERB scene ID) in lower panels. Ring in red shows limit of VZA =  $70^\circ$ .

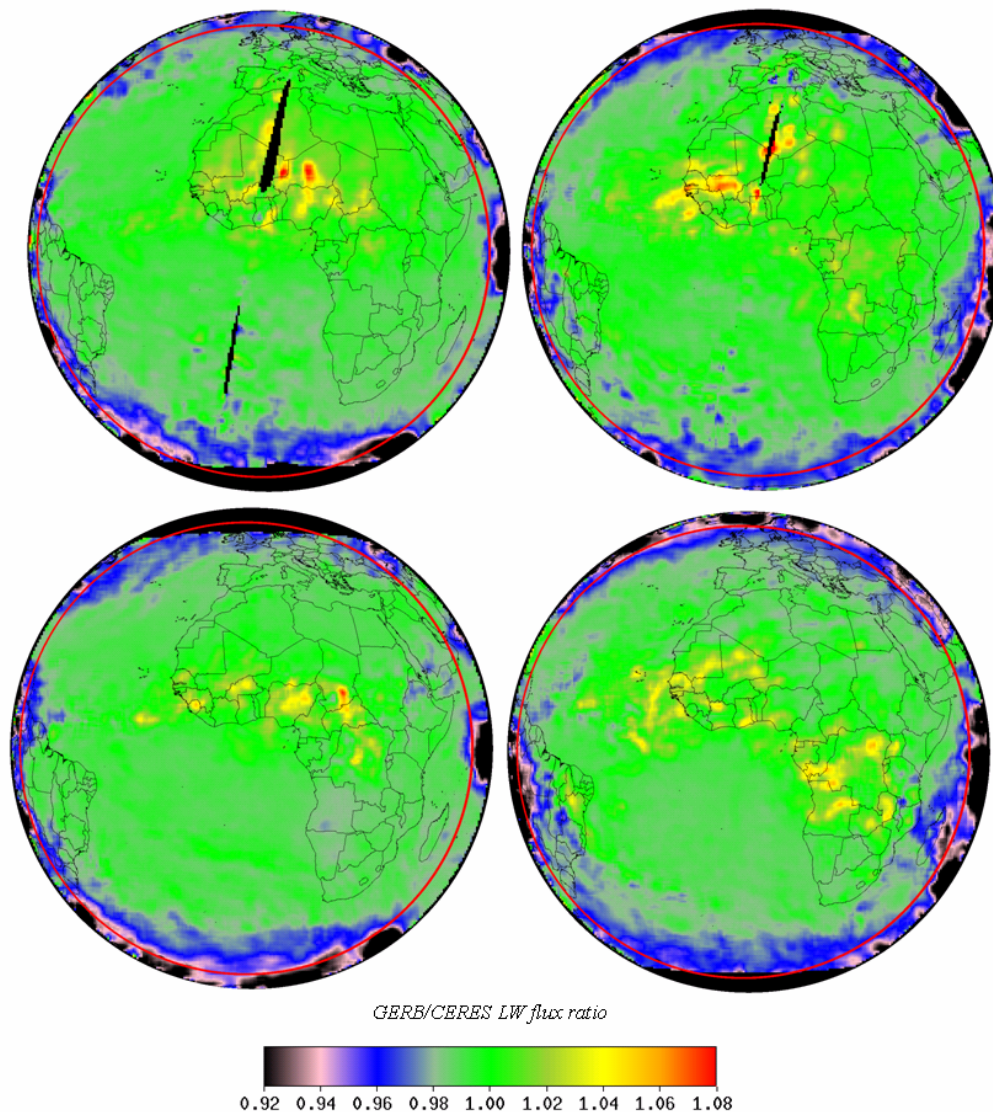


**Figure 3.** LW flux comparison for June (left) and December (right). GERB/FM2 ratio shown for day-time matches in upper panels and night-time matches in lower panels. Ring in red shows limit of VZA = 70°

## SUMMARY

Edition 1 GERB radiances and fluxes were released to the scientific community earlier this year. The stated absolute accuracy of these GERB radiances is 2.25% for the SW and 0.96% for the LW, where these are percentages of the typical full scale SW and LW values of  $240 \text{ Wm}^{-2}\text{sr}^{-1}$  and  $77 \text{ Wm}^{-2}\text{sr}^{-1}$  respectively. Comparisons between the GERB radiances and CERES FM2 radiances matched for time, location and viewing geometry indicate agreement to within the measurement errors (1% for GERB and 0.5% for CERES) in the LW. However GERB SW radiances are elevated with respect to CERES by on average 5% which is more than would be expected from their respective uncertainties in the SW (2.25% for GERB and 1% for CERES). Furthermore, consistent scene dependency in the SW comparison results is apparent, with greater percentage differences seen for dark scenes such as ocean than for bright scenes such as cloud. Possible causes of these differences are being investigated in both the CERES and GERB calibration and processing and the comparison methodology.

Comparisons between the GERB and CERES SW and LW fluxes, show that on average the GERB SW anisotropy factors are 1% higher than CERES for the same scene. This contributes to an elevation in the SW GERB/CERES flux ratio to 7% compared to the 5% seen for the SW radiance comparison. Scene dependent differences appear reduced in the SW flux comparison and there are few features in the geographic distribution of the GERB/CERES SW flux ratio except for some effects towards the edge of the disk, at coastlines due to geolocation errors and in the region of significant Saharan dust influence, which is believed to be due to the know issue of correctly accounting for aerosol.

Comparison of the LW fluxes shows similar average result to the overall GERB/CERES ratio found for the radiances, with GERB being about 1% lower than CERES. However a clear geographical pattern in the flux ratio is seen, with GERB radiances towards the limb of Earth, obtained at high viewing angles, being significantly lower than CERES. Conversely elevated GERB/CERES LW flux ratio are seen over regions subject to significant high thin cloud. These issues are believed to be associated with known issues with the GERB LW radiance to flux conversion factors as a function of viewing angle and for high thin cloud.

## REFERENCES

1. J E Harries, J E Russell, J A Hanafin, H Brindley, J Futyan, J Rufus, S Kellock, G Matthews, R Wrigley, A Last, J Mueller, R Mossavati, J Ashmall, E Sawyer, D Parker, M Caldwell, P M Allan, A Smith, M J Bates, B Coan, B C Stewart, D R Lepine, L A Cornwall, D R Corney, M J Ricketts, D Drummond, D Smart, R Cutler, S Dewitte, N Clerbaux, L Gonzalez, A Ipe, C Bertrand, A Joukoff, D Crommelynck, N Nelms, D T Llewellyn-Jones, G Butcher, G L Smith, Z P Szewczyk, P E Mlynczak, A Slingo, R P Allan and M A Ringer. The Geostationary Earth Radiation Budget Project. *Bull Am Met Soc*, 2005, Volume 86, No. 7, pp 945-960.
2. Schmetz. J. P. Pili, S. Tjemkes, D. Just, J. Kerkmann, S. Rota, A. Ratier, 2002: An introduction to Meteosat Second Generation (MSG). *Bull. Amer. Meteor. Soc.*, 83, 977-994
3. Munro R., A. Ratier, J. Schmetz, D. Klaes, 2002: Atmospheric measurements from the MSG and EPS systems. *Adv. in Space Res.*, 29, 1609-1618.
4. Loeb N. G., K. Loukachine K, N. Manalo-Smith, B. A. Wielicki, D. F. Young, 2003. Angular distribution models for top-of-atmosphere radiative flux estimation from the Clouds and the Earth's Radiant Energy System instrument on the Tropical Rainfall Measuring Mission satellite. Part II: Validation. *J Applied Meteorology* 42 (12): December 1748-176
5. Wielicki, B. A., B. R. Barkstrom, E. F. Harrison, R. B. Lee III, G. L. Smith, and J. E. Cooper, 1996: Clouds and the Earth's Radiant Energy System (CERES): An Earth Observing System Experiment, *Bul Am Met Soc*, 77, 853-868.